Supporting Information

Barg et al. 10.1073/pnas.1014823107

SI Text 1

Benefit of Solitary Granules. By analyzing only solitary granules, we hoped to distinguish the fluorescence that is spatially associated with granules and from that which is not. This strategy is now explored in computer simulations.

Clusters were modeled as Gaussian point-spread functions (Fig. S1*A*) and were added to random locations in an empty image (Fig. S1*B*) at a density ($1/\mu m^2$) similar to that observed in PC12 cells under total internal reflection fluorescence (TIRF) illumination. In this first simulation, all clusters were assumed to colocalize perfectly with granules of known locations. Gaussians with centers > 0.58 μm from that of any other Gaussian were selected, and images centered on such solitary Gaussians were averaged (Fig. S1*C*). As in Fig. S1*A*, there is a bright center, but it was surrounded by a dark ring and by fluorescence in the periphery. The peripheral fluorescence resulted from neighboring Gaussians, as it was increased when there were fivefold more Gaussians (Fig. S1*D*) but absent in the image of a single Gaussian (Fig. S1*A*). The dark ring resulted from imposing a minimum distance, because it became wider when the distance was increased to 0.85 μm (Fig. S1*E*), but vanished when it was reduced to zero, and all Gaussians in Fig. S1*B* were included in the average (Fig. S1*F*).

Line scans of Fig. S1 *A* and *C* may be compared in Fig. S1*J* (black curve and symbols, respectively). With increasing distance from the center, the light intensity drops then increases again to an asymptote. The theoretical value of the asymptote, 33.3 camera units (CU; dashed line) was calculated by multiplying the total light under the single Gaussian by the number of Gaussians per pixel.

As in experiments, images were analyzed with circle and annulus of the radii indicated in Fig. S1*J*, *Upper* (black for the circle and white for the annulus). In Fig. S1*A*, C = 109.4 CU and S = 2.9 CU; in Fig. S1*C*, C = 109.4 CU and S = 6.0 CU. Because there was no off-granule fluorescence in this simulation, the S values are spurious and represent stray light from the Gaussian in Fig. S1*A* and its neighbors. This small error makes our measurement of ΔF 3% too low (ΔF = 106.6 CU in Fig. S1*A* and 103.4 CU in Fig. S1*C*). A much larger error would result from choosing an annulus outside the granule-free zone.

In an otherwise identical simulation, we added granule-unrelated fluorescence in the form of randomly spaced Gaussians (density $3/\mu m^2$) (Fig. S1*G*). Averaged over the entire image, they contributed 99.8 CU. An average image (Fig. S1*H*) once again showed a bright center surrounded by a darker ring (see also red symbols and lines in Fig. S1*J*). ΔF was 101.8 CU essentially as in Fig. S1*C*, but all fluorescence values were now higher. In particular, S was 102.9 CU and within 3% of the theoretical value of the granule-unrelated fluorescence (99.8 CU, dotted line in Fig. S1*J*, and equal to the product of the number of granule-unrelated Gaussians per pixel and the light under a single Gaussian). In a third simulation, there was 15-fold more granule-unrelated than granule-related fluorescence, and the granule-related image was noisy (Fig. S1*I*). In the associated line scan (green in Fig. S1*J*), the granule-unrelated fluorescence (500.3 CU) is shown as a dotted line. Despite the large excess of granule-unrelated fluorescence, ΔF = 105.2 CU and S = 507.7 CU are both within 1.5% of their theoretical values. Finally, Fig. S1*K* plots a line-scan of an average syntaxin cluster in a live cell (see Fig. 1*C6*). Aside from a difference in amplitude, it is identical to the plots in Fig. S1*J*.

In summary, ΔF and S accurately measure the fluorescence of granule-related clusters and the granule-unrelated fluorescence that surrounds them, even if the latter is present in large excess.

SI Text 2

Diameter of Clusters and Granules in Fig. 1 *C5* and *C6*. Images of individual granules must be aligned before they can be averaged, as must images of clusters. The alignment of granules is accurate to within one pixel (89 nm), contributing to the image of a granule being more blurred than the point spread function (SD = 90 nm for a Gaussian fitted to the Airy disk calculated for NA = 1.45 and 610 nm). In addition, red and green optical channels must be brought into register; this also was done to within one pixel. Because Syx images are subject to two alignments and granules to only one, Syx images tend to be more blurred. The additional alignment counteracts the higher resolution provided by the shorter wavelength.

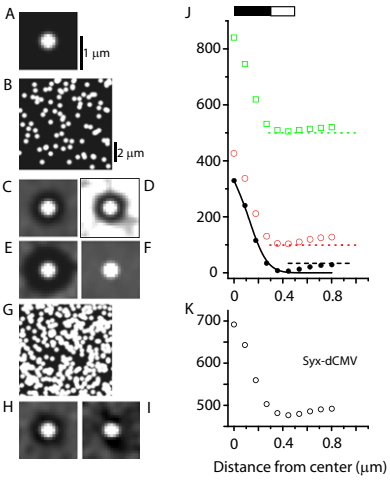

Fig. S1. On- and off-granule fluorescence analyzed in model images. (*A*) Image of a 2D Gaussian (peak fluorescence 327 CU, full width to half maximum, 0.30 μm) similar to the average on-granule cluster. Scale applies also to *C* to *F*, *H*, and *I*. (*B*) A total of 96 Gaussians added at random sites to an empty 110 × 110 pixel plane (area 95.8 μm^2). Scale also applies to *G*. (*C*) Averaged image centered on Gaussians in *B* that had no neighbor within 0.58 μm. Of the 1,920 Gaussians placed in 20 simulations, 689 qualified. (*D*) Simulation as in *B* but 480 Gaussians per plane. Of the 9,600 Gaussians placed in 20 simulations, 27 qualified and were located > 0.9 μm from the edge of the image. (*E*) As in *C*, but with a minimal distance of 0.85 μm and excluding Gaussians located <0.9 μm from the edge. (*F*) As in C, but including all 1,920 Gaussians. (*G*) Simulation as in *B*, but with an additional three Gaussians/μm^2 symbolizing off-granule clusters. (*H*) as in *C*, but from *G*. (*I*) Simulation as in *B* but with an additional 15 Gaussians/μm^2. (*J*) Linescans through the centers of the images *A* (black curve), *C* (black symbols), *H* (red symbols), and *I* (green symbols). Linescans were rotationally averaged after interpolation of pixel values. Red and green dashed lines show the granule-unrelated fluorescence; for black dashed line, see *SI Text 1*. (*K*) Linescan of Fig. 1 *C6*.

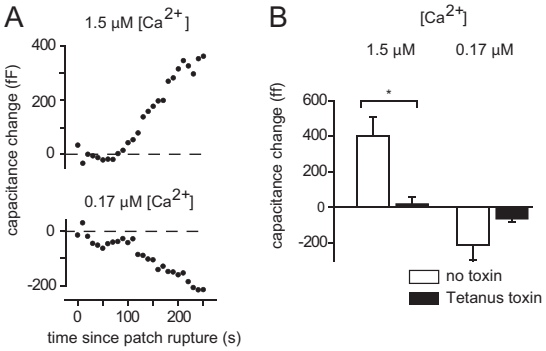

Fig. S2. Block of exocytosis by Tetanus toxin light chain (TeNT). Cells expressed Syx-GFP and NPY-mCherry, as judged by their fluorescence. Exocytosis was assayed by measuring the plasma membrane capacitance, a proxy for the cell surface area. A patch pipette containing solutions with 10 mM EGTA and strongly buffered concentrations of free [$Ca2^+$] (1.5 and 0.17 μM) was sealed against the plasma membrane. When the membrane patch beneath the pipette tip was ruptured, the solutions entered the cell and caused capacitance changes. (*A*) Capacitance in two cells, relative to its initial value, with [$Ca2^+$] as indicated. At 1.5 μM, the capacitance rose, indicating exocytosis; at 0.17 μM the capacitance declined, indicating endocytosis. The recordings and methods are similar to previous work on melanotropes (1) and chromaffin cells (2). (*B*) White bars, average from experiments as in *A*. Black bars, from similar experiments on cells transfected in addition with TeNT. Throughout, values are the difference in capacitance between 0 and 250 s after patch rupture. TeNT blocked the capacitance increase at 1.5 μM [$Ca2^+$] ($P < 0.01$, $n = 8$ each with and without TeNT). Results at 0.17 μM [$Ca2^+$] with and without TeNT were not statistically different ($n = 6$ each).

1. Thomas P, Surprenant A, Almers W (1990) Cytosolic Ca2+, exocytosis, and endocytosis in single melanotrophs of the rat pituitary. *Neuron* 5:723–733.
2. Augustine GJ, Neher E (1992) Calcium requirements for secretion in bovine chromaffin cells. *J Physiol* 450:247–271.

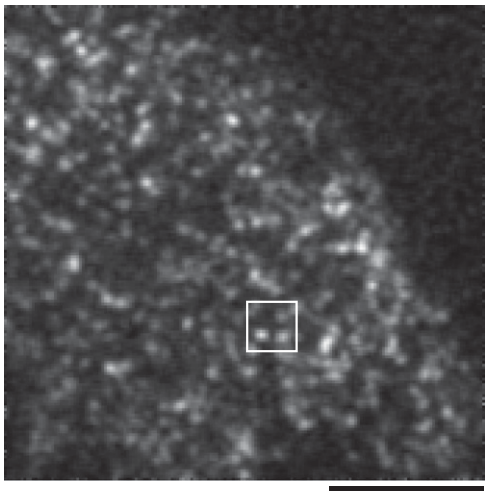

Movie S1. Fluctuating syntaxin clusters: 5-Hz recording of cell SB3186 in Fig. 4*A*. Movie was low-pass filtered (3 × 3 pixels) and is displayed on auto-scale to mitigate the effect of bleaching. Square indicates the position of images in Fig. 4*A*.

Movie S1